

Interaction of Two Perturbed Vortex Rings with Phase Difference

C.C.K. Tang, R.C.K. Leung and N.W.M. Ko

Department of Mechanical Engineering
 The University of Hong Kong
 Pokfulam Road, Hong Kong
 People's Republic of China

ABSTRACT

A numerical study of interaction of two coaxial weakly perturbed vortex rings with phase difference $\theta=90^\circ$ and without $\theta=0^\circ$ is reported. The model of the vortex rings is generated by thin vortex filament and their evolution is solved by means of three dimensional vortex blob method. Phase difference of the two vortex rings is an important parameter to their evolution and the slip through process.

INTRODUCTION

In free shear flow, such as circular jet, the research efforts concerned the investigation of the jet flow structures, their interaction and sound generation. The roll-up of the nozzle boundary layer into a train of coaxial ring vortices, their pairing and their eventual breakdown further downstream are the basic mechanism for the jet development. Recently, Leung and Ko [1] showed that the effect of perturbation on the interaction of two vortices is important in their evolution and the slip through process. The aim of this study is to further study the flow dynamics of two weakly perturbed vortex rings with and without phase difference.

NUMERICAL METHOD

Vortex Blob Method

The flow is assumed inviscid and incompressible. Each perturbed vortex ring is modelled by a slender vortex filament in unbounded space. The slender approximation, which ignores the role of core structure dynamics during the vortex evolution, gives only the global dynamics of the vortices and is a good candidate to study the long-wave behaviour of the vortex rings with perturbation. The three dimensional sinusoidal perturbation takes the form,

$$\mathbf{y} = (R + \rho_r e^{im\theta})\hat{\mathbf{e}}_r + (z + \rho_z e^{im\theta})\hat{\mathbf{e}}_z, \quad (1)$$

where \mathbf{y} is a point on the vortex filament, $\hat{\mathbf{e}}_r$ and $\hat{\mathbf{e}}_z$ the unit vectors in the radial and axial directions, m the wavenumber, θ the azimuthal angle, R the unperturbed ring radius and z the initial axial distance

from a frame to reference (Figure 1). As it is complicated to analyse the instability of vortex ring, which vortex core affects the self-induced motion of the vortex filament [2], a simple case is studied. The motion of vortex filament is approximated by means of vortex blob method [3,4]. The initial vorticity field is discretized into a collection of vortex vector elements [3], also called the vortex blobs, which are chosen to lie on the vortex filament, in the form

$$\boldsymbol{\omega}(\mathbf{y}, t) = \sum_{\alpha} \Gamma_{\alpha} \delta s_{\alpha} \zeta_{\sigma}(\mathbf{y} - \mathbf{y}_{\alpha}(t)), \quad (2)$$

where Γ_{α} is the circulation, \mathbf{y}_{α} the blob centre and δs_{α} the vector length of vortex blob. The spherically symmetric smoothing function ζ_{σ} , characterized by a smoothing radius σ , is constructed in the form $\zeta_{\sigma}(\mathbf{y}) = \zeta(|\mathbf{y}|/\sigma)/\sigma^3$, where $\zeta(\eta) = 15/(8\pi(\eta^2 + 1)^{7/2})$, with the three dimensional normalization $4\pi \int_0^{\infty} \zeta(\eta)\eta^2 d\eta = 1$. The smoothing radius is a numerical parameter introduced to inhibit the singular behaviour of the Biot-Savart Integral and should be of the same order of magnitude as the physical vortex core radius. In this study the constant smoothing radius was set equal to the physical vortex core radius. Hence, the discretized Biot-Savart velocity is given by

$$\mathbf{u}_{\alpha}(\mathbf{y}, t) = \frac{1}{4\pi} \sum_{\beta \neq \alpha} \Gamma_{\beta} \frac{\delta s_{\beta} \times (\mathbf{y}_{\alpha} - \mathbf{y}_{\beta})}{|\mathbf{y}_{\alpha} - \mathbf{y}_{\beta}|^3} \times \chi\left(\frac{|\mathbf{y}_{\alpha} - \mathbf{y}_{\beta}|}{\sigma_{\beta}}\right), \quad (3)$$

where $\chi(r) = 4\pi \int_0^r \zeta(\eta)\eta^2 d\eta$. The vortex filament is tilted and stretched by local velocity gradient $\nabla \mathbf{u}$ and these effects are accounted for in the change of vector length of the vortex blob, i.e. where $\mathbf{r}_{\alpha\beta} = \mathbf{y}_{\alpha} - \mathbf{y}_{\beta}$,

$$\frac{D\delta s_{\alpha}}{Dt} = \frac{1}{4\pi} \sum_{\beta \neq \alpha} \Gamma_{\alpha} \Gamma_{\beta} \left\{ \frac{|\mathbf{r}_{\alpha\beta}|^2 + \frac{5}{2}\sigma_{\beta}^2}{(|\mathbf{r}_{\alpha\beta}|^2 + \sigma_{\beta}^2)^{5/2}} \times (\delta s_{\beta} \times \delta s_{\alpha}) - 3(\delta s_{\alpha} \cdot \mathbf{r}_{\alpha\beta}) \frac{|\mathbf{r}_{\alpha\beta}|^2 + \frac{7}{2}\sigma_{\beta}^2}{(|\mathbf{r}_{\alpha\beta}|^2 + \sigma_{\beta}^2)^{7/2}} \times \right.$$

$$(\delta s_\beta \times \mathbf{r}_{\alpha\beta})\}. \quad (4)$$

The vortex blob representation of the Möhring's vortex sound formula could be similarly derived as

$$p(\mathbf{x}) = \frac{\rho_o}{12\pi c_o^2 |\mathbf{x}|^3} \frac{\partial^3}{\partial t^3} \left\{ \sum_\alpha \Gamma_\alpha \times (\mathbf{x} \cdot \mathbf{y}_\alpha) \mathbf{x} \cdot (\mathbf{y}_\alpha \times \delta s_\alpha) - \frac{1}{3} \sigma^2 \varepsilon \mathbf{x} \cdot \Omega \times \mathbf{x} \right\}, \quad (5)$$

where $\varepsilon = 4\pi \int_0^\infty \zeta(r) r^4 dr = 3/2$ and the total vorticity,

$$\Omega = \sum_\alpha \Gamma_\alpha \delta s_\alpha, \quad (6)$$

vanishes in unbound potential flow. The accuracy of numerical computation was governed by linear vorticity impulse,

$$I = \sum_\alpha \Gamma_\alpha (\mathbf{y}_\alpha \times \delta s_\alpha). \quad (7)$$

Due to the invariance of linear vorticity impulse, the circular axes of a perturbed vortex ring at a particular instant could be defined as a circular vortex ring having identical vorticity impulse at the instant, so that the shapes of the ring are constructed according to the equation

$$(0, 0, a) = \frac{\Gamma}{2} \int \left(\frac{\mathbf{y}(s) \times \partial \mathbf{y}(s) / \partial s}{|I|} \cdot \hat{\mathbf{I}} \right) ds, \text{ and} \\ \rho = \sqrt{\left(\frac{|I|}{\pi \Gamma} \right)}, \quad (8)$$

where ρ and a are the radial and axial position of the circular axis. The length and time are normalized by the initial condition of R_T and R_T^2/Γ_T respectively.

RESULTS AND DISCUSSION

Two perturbed vortex rings are shown in Figure 1. The quantities with suffixes L & T denote respectively the initially leading and initially trailing vortex rings. The ratio of vortex core radius to unperturbed ring radius was chosen to be 0.2. The circulation Γ is set at 1 at the start of simulation. Both radial and streamwise amplitudes of the weak perturbation wave were 0.02 times the unperturbed ring radius of the initially trailing vortex. The wave number m was set to 2 and the phase differences were chosen to be $\theta=0^\circ$ and $\theta=90^\circ$.

The radial accelerations of the two cases are shown in Figure 2. For both cases, during the first slip through at $2.4 < t' < 5$, the initially trailing vortex accelerates, while the initially leading vortex decelerates before the slip through instant at $t'=3.7$ (Figure 3). The accelerations of both vortices are the same for both cases. During the second slip through at $10 <$

$t' < 12.4$, there are differences that for $\theta=90^\circ$ the slip through instant occurs slightly later and their magnitudes are higher than those for $\theta=0^\circ$ (Figure 4). During the third slip through at $18 < t' < 20.4$, there are significant differences between the two cases. For $\theta=0^\circ$, the third slip through occurs at $t'=19.1$ and the rings are nearly perpendicular to each other, (Figure 5a). The maximum radial acceleration occurs at $t' \approx 19.1$, beyond which, due to the severely stretched and merging, computation was terminated. Thus, Figure 5b shows the two vortex rings at $t'=19.1$, before the third slip through. For $\theta=90^\circ$ the shape of the leading vortex (the initially leading vortex) does not vary greatly, while the trailing vortex (the initially trailing vortex) varies greatly in shape. The radial accelerations are different and occur later than those of $\theta=0^\circ$. Thus, the results indicate that due to the phase difference of the leading and trailing vortex rings, the evolution and the associated accelerations and decelerations of two rings are different from the second slip through.

CONCLUSIONS

The interaction of two weakly perturbed vortex rings with phase difference $\theta=90^\circ$ and without $\theta=0^\circ$ was studied by the vortex blob method. Numerical results show that three slip throughs are found for $\theta=0^\circ$, while only two slip throughs are obtained for $\theta=90^\circ$, before the termination of computation. There are also differences in the accelerations of the two rings from the second slip through.

ACKNOWLEDGEMENT

This work was supported by a grant from the Research Grants Council, Hong Kong.

REFERENCES

- (1) Leung, R.C.K., Ko, N.W.M.: "The interaction of perturbed vortex rings and its sound generation", *J. Sound Vib.* 202, (1997) pp.1-27.
- (2) Widnall Sheila E., Sullivan J.P.: "On the stability of vortex rings", *Proc. R. Soc. Lond. A.* 332, (1973) pp.335-353.
- (3) Knio, O.M., Ghoniem, A.F.: "Numerical study of a three dimensional vortex method", *J. Comp. Phys* 86, (1990) pp.75-106.
- (4) Winckelmans, G., Leonard, A.: "Contributions to vortex particle methods for the computation of three-dimensional incompressible unsteady flows", *J. Comp. Phys* 109, (1993) pp.247-273.
- (5) Möhring, W.: "On vortex sound at low Mach number", *J. Fluid Mech.* 85, (1978) pp.685-691.

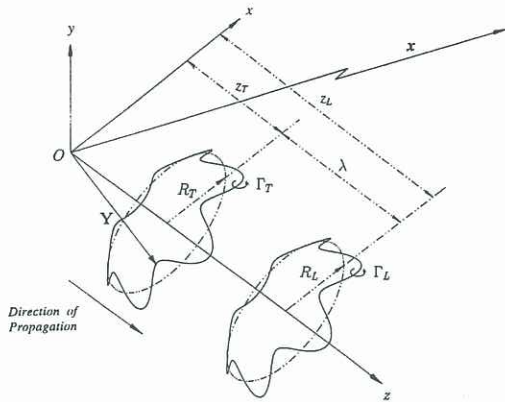


Figure 1: Schematic diagram of two perturbed vortex rings at start of simulation.

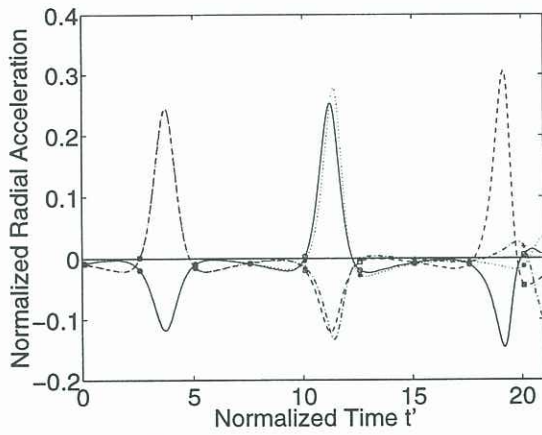
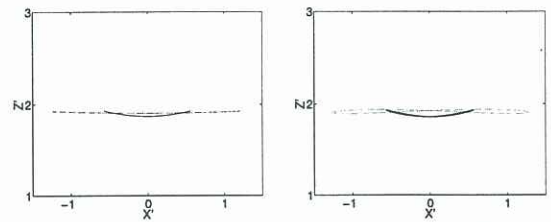
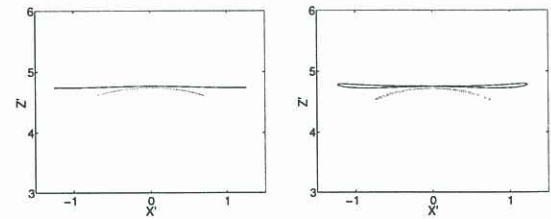


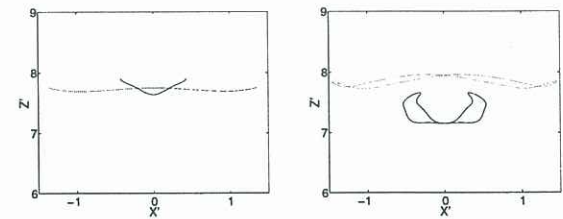
Figure 2: Temporal variations of radial accelerations. $m=2$.
 — Leading Vortex, $\theta = 0^\circ$;
 - - - Trailing Vortex, $\theta = 0^\circ$;
 Leading Vortex, $\theta = 90^\circ$;
 - · - · Trailing Vortex, $\theta = 90^\circ$.



(a) $\theta = 0^\circ$ (b) $\theta = 90^\circ$
 Figure 3: First slip through instant $t'=3.7$.
 Initially leading vortex;
 — Initially trailing vortex.



(a) $\theta = 0^\circ$ (b) $\theta = 90^\circ$
 Figure 4: Second slip through instant $t'=11.1$.
 Initially leading vortex;
 — Initially trailing vortex.



(a) $\theta = 0^\circ$ (b) $\theta = 90^\circ$
 Figure 5: Third slip through instant $t'=19.1$.
 Initially leading vortex;
 — Initially trailing vortex.